JOURNAL OF COMPUTATIONAL PHYSICS 7, 465–488 (1971)

Relative Stabilities of a Family of Plastically-Deformed Lattice Close Packings of Rigid Disks

C. GRANT MILLER AND RUSSELL D. LARSEN

Department of Chemistry, Illinois Institute of Technology, Chicago, Illinois 60616

Received October 27, 1970

Using the cell-cluster approximation scheme we have ascertained the relative stabilities of a family of plastically-deformed lattices containing interacting rigid disks. These lattices, referred to as Niggli lattices, represent a distortion of the regular hexagonal lattice in that single rows are systematically translated away from hexagonal packing to yield interpenetrating parallelopipedal unit cells. The cell-cluster analysis has been taken only through second order due to the complexity of the resulting subfigures. However, the results have been parameterized in terms of general translation variables which permits us to display the contents of the correlated configurational regions for all members of the infinite set of such row translates or Niggli-type lattices. In this regime we are no longer able to determine limiting contents which are exact in the close-packed limit; rather, we construct bounds to such exact regions.

I. INTRODUCTION

The cell-cluster theory represents a powerful approach to a systematic evaluation of the N-particle, classical configurational partition function for hard-sphere systems. Furthermore, this technique in the asymptotic limit of $V \to V_0$, the close-packed volume, yields results which are exact through each order and thus provides a formalism for a detailed study of the ideal, anharmonic crystal.

In general, actual physical systems will not correspond to this model system of an ideal crystal but will contain s-dimensional lattice defects corresponding, for example, to vacancies and divacancies ($s = 0$), dislocations ($s = 1$) and grain boundaries ($s = 2$). The bulk properties of the physical system will, of course, reflect the presence of such imperfections. As yet, no statistical mechanical model has been developed which is capable of considering all of these divergences from perfect crystalline behavior inasmuch as the ideal crystal is still incompletely characterized due to the nature of the many-body problem for strongly interacting systems. Ideally, such a general model would enable us to calculate macroscopic properties of imperfect, disordered systems by enabling us to calculate exactly, or estimate in some accurate yet convenient form, the configurational partition

function and pair distribution function. The cell-cluster approximation scheme is capable of assuming a central role in such a program.

There is a great wealth of solid state phenomena that may be studied within the context of a lattice model of interacting hard-particle systems and the cell-cluster scheme. The formalism has been applied successfully, for example, to such equilibrium problems as the formulation of a high-density expansion of the free energy analogous to the low-density virial expansion and to the determination of the elastic constants of such high-density crystalline systems.

Our program is concerned with the characterization of the statistical mechanics of fracture and embrittlement phenomena, both being of considerable technological and engineering interest. Our viewpoint is that such material-failure phenomena are themselves many-body, cooperative events which may be characterized to first order by classical statistical mechanics using a lattice model with particles interacting via purely repulsive potentials. Considered from this point of view, fracture and embrittlement have much in common with melting and the ubiquitous problem of crystalline stability. In terms of such a lattice model we may consider that there are lattice configurations which, at equilibrium, have a relative stability which is a function of packing arrangement as well as of the presence and concentration of lattice defects. The calculation described herein was undertaken in an attempt to understand the contribution made by geometric configuration and a plastic deformation thereof to crystalline stability in the absence of an explicit external stress field.

We consider a family of two-dimensional lattices that are close-packed lattices (one member being the highest-density hexagonal lattice) which correspond to a continuous plastic deformation of one configuration to another. Our interest is in the relative stability of these lattices at equilibrium. The approach described here is not specific to the lattice configurations and calculations presented but is capable of treating a wide variety of crystalline systems. We have employed the same analytic-geometric techniques that were previously developed [1] in order to ascertain the correlated content of multidimensional regions of configuration space accessible to interacting rigid particles on a lattice.

II. Cell-Cluster Expansion of The Helmholtz Free Energy for Plastically-Deformed Hexagonal Lattices

A. *Introduction*

The cell-cluster expansion technique for hard-particle systems has been described in detail in earlier work [2, 3]. The scheme may be applied to either the configurational partition function or to the Helmholtz free energy. We work within the

context of the latter inasmuch as the successive correction terms contributing to the N-particle Helmholtz free energy, A_N, are most easily visualized for the free energy itself.

We consider a family of N-particle systems, each member spanning a different virtual lattice. For each sphere system/lattice we consider all distinct nearest-neighbor pair interactions and denote the set of such interactions by $\{(n, t)\}$. Each element of this set is referred to as a cell-cluster of n-particles and topological configuration t. In considering the pair-wise interaction of n-particles within a cluster the remaining $(N - n)$ particles are constrained to their lattice sites but delimit the accessible configurations of the particles within the cluster. In order to ascertain the contribution of a given cluster (of rigid disks of diameter σ, for example) to the free energy, it is necessary to evaluate the canonical configurational partition function $Q_{n,t}$ which may be expressed as

$$Q_{n,t} = \int_{\mathscr{R}_{n,t}} \cdots \int \prod_{i<j} A(R_{ij} - \sigma) \prod_{i=1}^{n} d\mathbf{R}_i , \tag{1}$$

where R_{ij} is the distance between centers of an (ij) pair, the integration is over a specific convex region $\mathscr{R}_{n,t}$ of configuration space of exact content $\mathscr{V}_{n,t}^{(2)}$, and $A(x)$ is the unit step function. The contribution to the Helmholtz free energy A_N of a specific cell cluster (n, t) is then

$$A_{n,t}/k_B T = -\ln(Q_{n,t}/n!\, \Lambda^{2n}), \tag{2}$$

where

$$\Lambda = h(2\pi m k_B T)^{-1/2}.$$

The N-particle free energy being composed of weighted contributions from each member of the set $\{(n, t)\}$ may be written as a sum of successive correction terms, $W_{n,t}$, each $W_{n,t}$ correcting $Q_{n-1,t}$ for the presence of n-particle interactions:

$$A_N/Nk_B T = \sum_{n=1}^{N} \sum_{t} g(n, t)\, W_{n,t} . \tag{3}$$

The combinatorial factor, $g(n, t)$, arises from the fact that the system of N particles may be partitioned into clusters (n, t) in $Ng(n, t)$ different ways. The prescription for obtaining the successive $W_{n,t}$ functions is provided by a recursion relation:

$$\begin{aligned} W_{1,1} &= A_{1,1}/k_B T, \qquad n = 1, \\ W_{n,t} &= (A_{n,t}/k_B T) - \sum_{i=1}^{n-1} \sum_{j=1}^{T_i} C_{n,t}^{i,j} W_{i,j} , \qquad n \geqslant 2, \end{aligned} \tag{4}$$

where $C_{n,t}^{i,j}$ is the combinatorial factor giving the number of figures of type (i, j) contained in (n, t). These combinatorial factors are different for each member of the family of lattices which we consider. T_i is the number of different configurations of a connected subfigure of i particles.

B. *Niggli Lattice I*

We shall consider in detail three members of a family of the infinite set of plastically-deformed hexagonal lattices and discuss the coordinate systems used for each in carrying out the $Q_{n,t}$ integrations. For illustrative purposes we refer specifically to two classes of these lattices as Niggli Lattices I and II [4]. The third member is the familiar undistorted regular-hexagonal lattice which has been previously characterized in detail in earlier work [2, 3]. Niggli Lattice I is actually a member of a class of asymmetric 5-coordinate, 2-dimensional lattices with B^2 sites, i.e., B rows of B sites per row. A close packing of rigid disks on such a lattice is shown in Fig. 1. Also shown are the resulting Voronoi polytopes and dual lattice

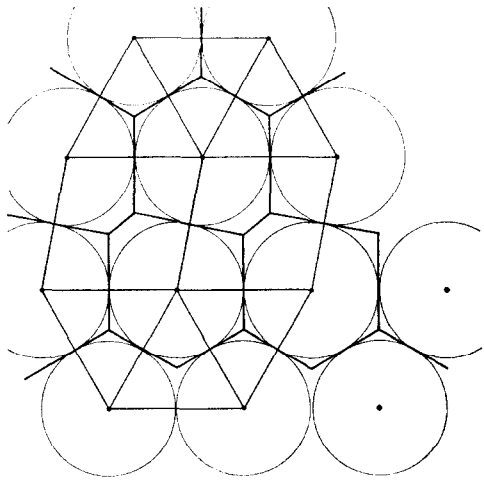

FIG. 1. Niggli Close Packing of Rigid Disks, I. Asymmetric Hexagonal Voronoi Polytopes and Dual Lattice of Triangles and Quadrilaterals.

consisting of triangles and quadrilaterals. The lattice sites may be defined in terms of the basis vectors $\mathbf{a}_1$ and $\mathbf{a}_2$ of the parallelopipedal unit cells which are depicted in Fig. 2. Inasmuch as Niggli I is not a Bravais lattice but rather a lattice-with-a-basis a lattice translation about the two distinct sites of the unit cell

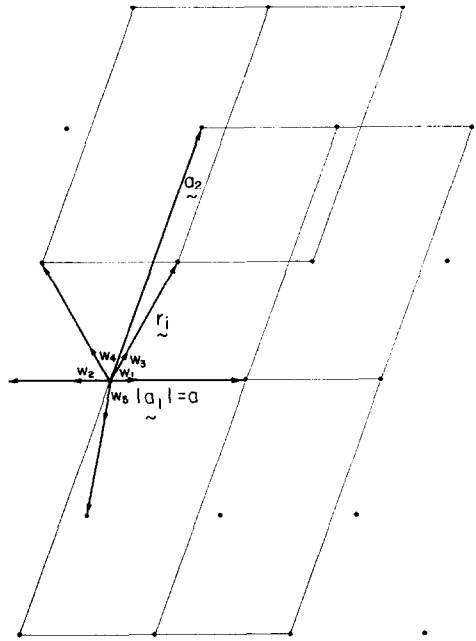

FIG. 2. Parallelopipedal unit cells of Niggli Lattice I showing interpenetrating simple lattices.

generates two parallel and interpenetrating simple lattices the lattice sites of which are defined by

$$\mathbf{R}^0_{q,\alpha} = \mathbf{r}_q + \sum_{j=1}^{2} \alpha_j \mathbf{a}_j \qquad (q = 1, 2), \tag{5}$$

$$\alpha = \{\alpha_1, \alpha_2\} \text{ are integers } = 0,..., B - 1,$$

$$| \mathbf{a}_1 | = a.$$

Each simple unit cell q is specified by the primitive translations $\mathbf{a}_j$.

The unit vectors between nearest-neighbor lattice sites may be expressed as

$$\begin{aligned} \mathbf{w}_1 &= -\mathbf{w}_2 = \mathbf{a}_1/a, \\ \mathbf{w}_3 &= (\mathbf{a}_1 + \mathbf{a}_2)/2a, \\ \mathbf{w}_4 &= (\mathbf{a}_2 - \mathbf{a}_1)/2a, \\ \mathbf{w}_5 &= (\lambda_1 \mathbf{a}_1 - \lambda_2 \mathbf{a}_2)/a. \end{aligned} \tag{6}$$

Niggli I is a specific lattice for which $\lambda_1 = -3/16$ and $\lambda_2 = -1/2$. The system of

vectors $\{\mathbf{a}_j\}$ is not orthonormal and may be transformed into a reciprocal basis $\{\mathbf{b}_m\}$ which is often more convenient for actual computational purposes. However, due to the asymmetry of the Niggli I lattice, an oblique, reciprocal basis such as was used with the regular hexagonal lattice calculations in previous work [2, 3] is no more advantageous than the rectangular Cartesian system which has been employed herein.

Consider now a close packing of rigid disks on Niggli Lattice I. The configurational partition function for such a system of 2-spheres may be approximated by a cell-cluster analysis. The nature of the lattice and pair-wise interactions involved is best seen by considering the region of configuration space $\mathscr{R}_1$ containing particle 1 defined by

$$Q_1 = \int_{\mathscr{R}_1} \cdots \int \prod_{1<j} A(R_{1j} - \sigma)\, d\mathbf{R}_1 . \tag{7}$$

The exact configurational partition function for such a single-particle (singly occupied) cell is thus defined by the area of one of the irregular five-sided regions bounded by circular arcs as depicted in Fig. 3. These regions represent the "free area" to which the center of a particle has access, subject to the hard-particle nonoverlap restriction. Asymptotically, in the close-packed limit, $V \to V_0$, within which we shall be working, the circular arcs are replaced by their tangent hyperplanes and the integral Q_1 is able to be represented by the area of an irregular

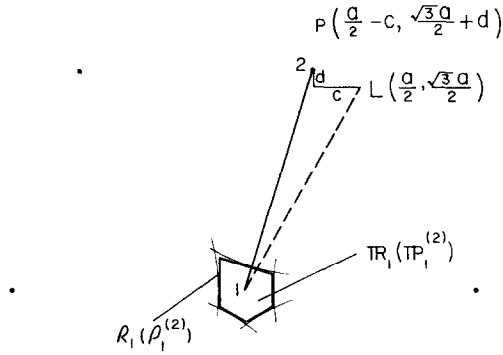

FIG. 3. Exact irregular pentagonal region $\mathscr{R}_1$ having hypercylindrical boundaries and limiting planar pentagonal bound $\mathbb{R}_1$ for a singlet cell of Niggli Lattice I.

pentagon $\mathbb{R}_1$, of content $\mathbb{P}_1^{(2)}$ as shown in Fig. 3. It is apparent from this figure that all such areas are of the same conformation, though their orientations differ.

Figure 1 also serves to illustrate how Niggli Lattice I is built up from alternating rows of hexagonal packing and rows of translated or distorted hexagonal packing. For example, if rows 1 and 2 are hexagonally packed with respect to one another, then rows 3 and 2 are "distorted" by a translation of rows 3 and 4 away from the nominal hexagonal lattice sites such that rows 3 and 4 still remain hexagonally packed with respect to each other. The entire lattice is constructed in this manner by alternating pairs of hexagonally-packed rows with pairs of rows having "distorted" packing. It remains to characterize and parameterize the nature of a general distortion such as between rows 3 and 2. With such a general characterization the lattice structures for a family of such packings will have been specified.

It is our purpose to characterize as general a distortion a possible, so that, within the framework of our development, we may easily vary the nature of the distortion to determine its effect on the configurational partition function Q_1 and the "relative stability" of the lattice. Figure 3 illustrates, in a rectangular coordinate

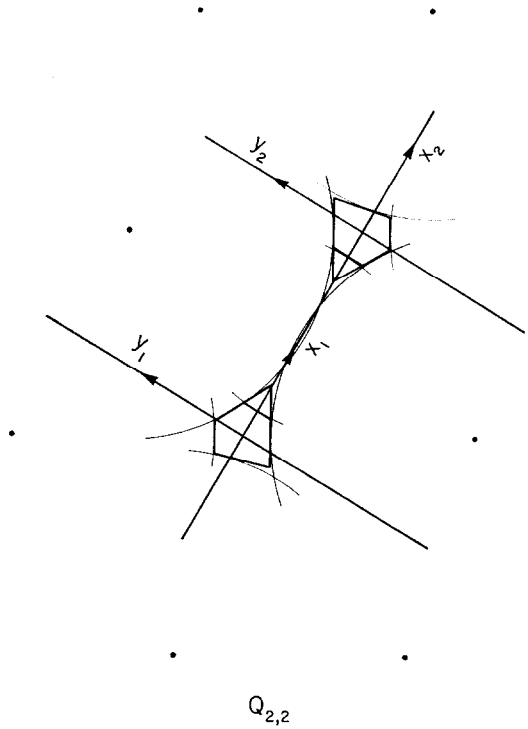

FIG. 4. Pair cell-cluster $Q_{2,2}$ of Niggli Lattice I.

system, the parameters necessary for such a development. The centers of two rigid disks on Niggli Lattice I denoted by points 1 and 2 represent a distortion or translation with respect to each other from the regular hexagonal lattice. All particles which are distorted relative to one another for this specific lattice structure conform to this configuration. Point L refers to the nominal position of a lattice site of the regular hexagonal lattice (relative to Point 1) whereas Point P refers to the position of a lattice site of Niggli Lattice I obtained by a translation (distortion) of an entire row from, for example, sites represented by $\{L\}$ to those represented by $\{P\}$. The distortion is parameterized by a displacement of Center 2 by (1) a general distance (c) in the negative x direction, and by (2) a general distance (d) in the positive y direction. With (c) and (d) as variables, we define an entire family of such distorted lattices. All interactions and correlated areas necessary for the determination of the $Q_{n,t}$ are described solely in terms of the distances c, d, a (distance between lattice sites) and $(a - \sigma)$, the "radius" of an irregular pentagonal singlet cell as in Fig. 3.

In the high-density limit, the configuration integral $Q_1(\mathscr{P}_1^{(2)})$ is approximated by the content $\mathbb{P}_1^{(2)}$ of one of the irregular pentagons $\mathbb{R}_1$ shown in Fig. 3. $Q_1{}^N(\mathbb{P}_1^{(2)})$ then represents the limiting cell-model approximation to Q_N for this lattice/disk system. By considering Q_2 we may correct the independent-particle cell approximation for the correlation of disk pairs. Considering a specific two-particle correlation such as depicted in Fig. 4, if Particle 1 moves to a position so that the x component of its vector position is negative, then Particle 2 may move toward Particle 1 in the $-x_2$ direction so that it is beyond the nominal single-particle "free area" yet correlated as a nearest neighbor to Particle 1. The multiplicity of such correlations for these asymmetric configurations considerably complicates a pure analytical treatment. Herein we present only the results and contributions of such pair correlations. Using a polytope bound analytic integration routine such as the exponential polynomial integration by-parts algorithm developed by the Salsburg group at Rice University [5], we may also consider the variety of triplet and higher-order interactions that arise for these lattices. We should hope to be able to improve the bounds through second order, however, in addition to considering such higher order interactions.

The multiplicity of correlated-pair allowed regions of configurations space is shown in Fig. 5. There are four such distinct correlated areas that must be distinguished, and these are labelled topologically as $Q_{2,1}$, $Q_{2,2}$, $Q_{2,3}$ and $Q_{2,4}$ in Fig. 5. Inasmuch as

$$Q_{2,t} = Q_1{}^2 + W_{2,t} \tag{8}$$

or

$$W_{2,t} = Q_{2,t} - Q_1{}^2, \tag{9}$$

then

$$A_N \cong NA_1 + \sum_{t=1}^{4} g_{2,t} W_{2,t} , \tag{10}$$

where $g_{2,t}$ is a combinatorial factor depending directly upon a specific pair configuration t.

We have thus characterized a generalized continuous distortion corresponding to the class of lattices of type denoted as Niggli Lattice I, the nearest-neighbor unit vectors of which are given by Eq. (6). Such a specific lattice gives rise to an approximation to A_N, Eq. (10), which considers the multiplicity of pair correlations implicit in the $Q_{2,t}$ functions. We have previously presented an analytic-geometric approach to this type of calculation [1]. The methods used here closely parallel

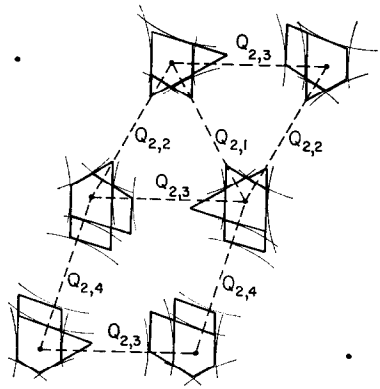

FIG. 5. Bounds to pair subfigures $Q_{2,t}$ of Niggli Lattice I.

those presented therein. Since the actual analytic computational procedure is quite complicated and tedious, we display the explicit evaluation of Q_1 and $Q_{2,2}$ in Appendix I. These calculations are illustrative of the procedures followed and while $Q_{2,2}$ is the most difficult of the four $Q_{2,t}$ functions to evaluate, its presentation serves to illustrate all of the problems encountered. We merely cite the results for $Q_{2,1}$, $Q_{2,3}$, and $Q_{2,4}$ here.

In Appendix I, general expressions for Q_1 and $Q_{2,2}$ appear which depend solely on the quantities a, σ, c and d. Specific numerical values for Q_1 and $Q_{2,2}$ arise if we arbitrarily choose: $a = 8$, $\sigma = 7$, $c = 1$, $d = 0.5$. Note that $(a - \sigma) = 1$, as in previous work with the regular hexagonal lattice [2, 3]. The specification of these values corresponds to the choice implied in Fig. 3. With the specification of these parameters we delimit a specific lattice and define a close packing of disks on such a lattice for which

$$\begin{aligned} Q_1 &= 3.16, \\ Q_{2,1} &= 10.69, \\ Q_{2,2} &= 10.99, \\ Q_{2,3} &= 12.18, \\ Q_{2,4} &= 15.50. \end{aligned}$$

Recall that for the regular hexagonal lattice,

$$\begin{aligned} Q_1 &= 3.00, \\ Q_{2,1} = Q_{2,2} &= Q_{2,3} = Q_{2,4} = 9.042. \end{aligned}$$

The correction factors $W_{n,t}$, for Niggli Lattice I are obtained from Eq. (9) as

$$W_{2,1} = .70, \qquad W_{2,2} = 1.00, \qquad W_{2,3} = 2.19, \qquad W_{2,4} = 5.51.$$

The free energy function A_N may be written in terms of the $W_{n,t}$ as in Eq. (10), given the combinatorial factors $g_{n,t}$. Each rigid disk has two pair interactions of the type $Q_{2,3}$ and one each of the types $Q_{2,1}$, $Q_{2,2}$, $Q_{2,4}$. Inasmuch as there are 5 pair interactions altogether for N disks, the total number of distinct interactions is $5N/2$. These are accordingly distributed as $g_{2,1} = N/2$, $g_{2,2} = N/2$, $g_{2,3} = N$, $g_{2,4} = N/2$, thus permitting evaluation of Eq. (10) through second order. It has been conjectured, however, that the Helmholtz free energy possesses the following asymptotic expansion [3]:

$$A_N/Nk_BT \sim 2\ln(\lambda/\sigma) - 2\ln(\theta^{-1} - 1) + C + O(\theta^{-1} - 1), \tag{11}$$

where θ is a reduced density variable

$$\theta = \sigma^2/a^2$$

and C is the additive free energy constant

$$C = C_{fv} - \sum_{n=2}^{N} \Big[\sum_t g(n, t) \ln Y_{n,t}\Big], \tag{12}$$

$$Y_{n,t} = \exp[-W_{n,t}/k_BT].$$

For lattice packings such as we are considering here such an asymptotic expansion must be generalized in order to account for the possibility that a lattice will consist of interacting nearest-neighbor pairs which are separated by a distance $a(n, t)$ which is not invariant but a function of a specific pair interaction. Consider Fig. 5, for example. We have depicted the pair subfigures for a specific member (Niggli I) of a general family of lattices for which $a(2, 1) = a(2, 2) = a(2, 3) \neq a(2, 4)$. Thus, the reduced density variable θ in this case depends on the weighting factor $g(n, t)$. For a distorted or plastically-deformed lattice we may write the free energy per particle as

$$A_{\text{Niggli}}/Nk_BT \sim 2\ln(\lambda/\sigma) - 2\sum_n \sum_t g(n, t) \ln(\theta^{-1}(n, t) - 1) + C' + \cdots, \quad (13)$$

where C' now includes the constant terms which arise from $\ln(\theta^{-1}(n, t) - 1)$, where

$$\begin{aligned} \theta^{-1}(n, t) &= \theta^{-1} + \delta(n, t) \\ \theta &= \sigma^2/a^2 \end{aligned} \quad (14)$$

and

$$C' = C_1 - \sum_{n=2}^{N} \left[\sum g(n, t) \ln Y'_{n,t}\right], \quad (15)$$

where

$$Y_{n,t} = Q_{n,t}(\text{Niggli})/Q^2_{n-1}(\text{Hex}), \qquad n = 2. \quad (16)$$

Equation (13) represents an expansion of the free energy about that of the undistorted hexagonal lattice. Equations (15) and (16) are a natural consequence of this expansion procedure.

C_1 is the value of $C_{n,t}$ obtained by considering the single-particle *undistorted* "free area" which is .144. The value of C' is, of course, different for each member of the family of lattices. For Niggli Lattice I we obtain $C_2' = -.599$ through order $n = 2$. A discussion of this result is postponed until we have considered Niggli Lattice II in the next section.

C. *Niggli Lattice II*

The results outlined in the previous section represent the characterization of a typical intermediate distortion—one member of a class of possible such distortions (row translations or plastic deformations). It is interesting to note the results of the extremal distortions. One end of the spectrum of distortions obtainable under this regime is represented by the undistorted regular hexagonal lattice which has been previously considered. We have merely cited the results previously obtained for it.

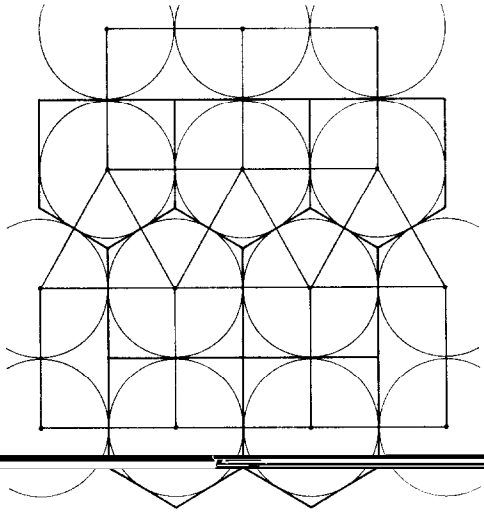

FIG. 6. Niggli Close Packing of Rigid Disks, II. Symmetric Pentagonal Voronoi Polytopes and Dual Lattice.

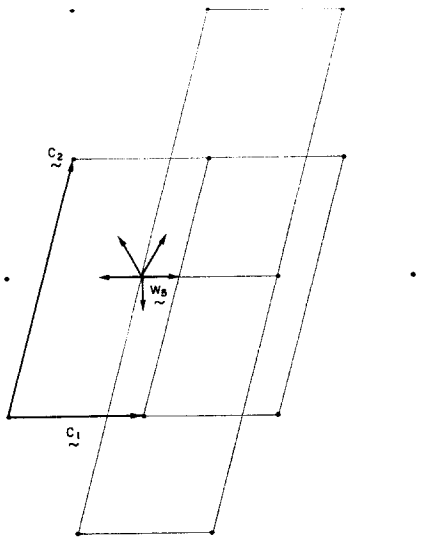

FIG. 7. Parallelopipedal unit cells of Niggli Lattice II showing interpenetrating simple lattices.

Another extremal distortion (maximum distortion in the direction c) is represented in Fig. 6. We refer to this lattice as Niggli Lattice II. It is again a lattice-with-a-basis for which there are two distinct sites for a parallelopipedal unit cell as shown in Fig. 7. Thus, a lattice translation about these sites also generates two parallel and interpenetrating simple lattices defined by Eq. (5) in terms of the primitive translations $\mathbf{a}_j$. The unit vectors between nearest-neighbor sites of Niggli II may be expressed by Eq. (6) except that for $\mathbf{w}_5$ the parameters λ_1 and λ_2 are specifically

$$\lambda_1 = 0 \qquad \text{and} \qquad \lambda_2 = -1/\sqrt{2 + \sqrt{3}}.$$

The calculations of Q_1 and $Q_{2,t}$ for this lattice are considerably more simple than the corresponding calculations for Niggli Lattice I. The extreme nature of the distortion results in the displacement of a row of particles by exactly one-half of the interparticle distance so that distorted particles are directly in line with undistorted particles (as reflected by $\lambda = 0$). This introduces an element of symmetry lacking in Niggli I which greatly facilitates the calculations. Furthermore, the number of distinct two-particle subfigures is reduced from four for Niggli I to three for Niggli II. Appendix II outlines the necessary computations for this lattice configuration. The results are expressed as

$$\begin{aligned} Q_1 &= 2.50, \\ Q_{2,1} &= 9.96, \\ Q_{2,2} &= 11.72, \\ Q_{2,3} &= 5.88, \\ C_1 &= .144, \\ C_2' &= .340. \end{aligned}$$

These results and the results for Niggli Lattice I differ significantly from the results obtained for the undistorted hexagonal lattice. Corresponding to the usual interpretation of C, the large negative result for Niggli Lattice I, ($C_2' = -.599$), indicates a dramatic increase in the stability of the lattice in comparison to the hexagonal, undistorted lattice ($C = .130$) [2]. On the other hand, the large positive result for Niggli Lattice II, ($C_2' = .340$) indicates a decrease in the stability of that lattice relative to the hexagonal, undistorted lattice. This surprising result, i.e., two highly distorted lattices exhibiting very different apparent stabilities is a consequence of the rigid-disk model itself.

A rigid-particle/lattice model assumes only short-range repulsive forces between particles. As such, this model is expected to be valid in the close-packed limit where the repulsive interparticle forces predominate. If a particle separation away from closest packing is introduced, there will be a decrease in the importance of the

repulsive forces between particles whereupon the model is expected to manifest a greater stability such as is observed in Niggli Lattice I. Niggli Lattice II was constructed such that the pair function $Q_{2,2}$ of Fig. 9 assumes a minimal interparticle separation. This destabilizes Niggli Lattice II, ($C_2' = .340$), by emphasizing the short-range repulsive interparticle forces.

Thus, the C' notation is sufficient to low order ($n = 2$) to characterize the stability of a lattice due to short-range repulsive interactions.

A more comprehensive theory should be able to take into account destabilization due to interstitial voids, grain boundaries, and other defects. Theoretically, these phenomena may be investigated within the cell-cluster scheme by calculating the higher-order contributions ($n = 3, 4,...$) which comprise C'. For the distorted lattices considered herein such calculations are difficult and we seek an alternative method which may be applied to low order.

The stability of a lattice is inherently related to lattice distortion through two effects: (1) compression of the particles yielding a destabilization through interparticle repulsion at short-range and, (2) the production of interstitial voids. While C' is a good measure of the first, it is not a good measure of the second to low order. Interstitial void destabilization is undoubtedly related to the number density of a lattice, for the greater the amount of void space the less the density of the lattice. However, it is apparent that both Niggli I and Niggli II have number densities less than that of the hexagonal lattice, and yet the results for these two lattices differ markedly.

We can relate, however, the interstitial void space to the $Q_{2,t}$ functions—the greater the amount of void space in a lattice the greater the area over which the center of a particle may wander for configurational interaction. Thus, a large amount of void space necessarily must produce a large value of $Q_{2,t}$. Such large values of $Q_{2,t}$ produce large negative contributions to C' and, consequently, tend to decrease the free energy of the lattice (cf., Eq. (14)). Lattice compression will give smaller pair-configurational functions $Q_{2,t}$ and thus large positive contributions to C'.

We suggest that the additive free-energy constant of the undistorted hexagonal lattice ($C = .130$) represents, in some sense, a standard of stability. Those lattices which have a value significantly greater than this value (such as Niggli Lattice II) manifest considerable destabilization due to lattice compression. Those lattices which produce a value significantly less than this value (such as Niggli Lattice I) manifest destabilization due to interstitial void space. Thus we suggest it is the *magnitude* of C' which denotes destabilization and the sign of C' designates whether this destabilization is due to lattice compression or interstitial void space. Further, it is possible to imagine a lattice which would contain destabilizing contributions due to both compressive and void effects so that the free energy would be of the magnitude of that for the hexagonal undistorted lattice, whereas, in reality, the

lattice would be quite unstable. In such a case the contributions from the $Q_{2,t}$ would be both large positive and large negative while their total contribution to C' would largely cancel each other. It is tempting to consider a sum of the positive $Q_{2,t}$ to represent destabilization due to compression and of the negative $Q_{2,t}$ to represent destabilization due to interstitial void space. Carried to its logical extreme, this formulation would be lead to a phenomenology of lattice distortion, each distortion being a function of both characteristic compressive and void instabilities characterized by the $Q_{2,t}$ and their contributions to C'. Thus we may write Eq. (15) in the form

$$C' = C_1 - C_c - C_s ,$$

where

$$C_c = \sum_{n=2}^{N} \left[\sum_{t_c} g(n, t_c) \ln Y'_{n,t} \right],$$

$$C_s = \sum_{n=2}^{N} \left[\sum_{t_s} g(n, t_s) \ln Y'_{n,t} \right],$$

and the t_c are those configurations for which $(\ln Y'_{n,t}) \geqslant 0$, and the t_s are those configurations for which $(\ln Y'_{n,t}) < 0$.

Then $C_2(\text{Hex}) - C_c$ is a measure of destabilization due to lattice compression and $C_2(\text{Hex}) - C_s$ is a measure of destabilization due to interstitial void space.

For Niggli Lattice I, we obtain

$$\begin{aligned} C_1 &= .144, \\ C_s &= +.743, \\ C_c &= 0.0, \\ C_2' &= -.599, \end{aligned}$$

and for Niggli Lattice II, we obtain

$$\begin{aligned} C_1 &= .144, \\ C_s &= .235, \\ C_c &= -.431, \\ C_2' &= .340. \end{aligned}$$

The magnitude and sign of these contributions is consistent with the above interpretation.

APPENDIX I: GENERAL RELATIONS FOR THE CONFIGURATIONAL PARTITION FUNCTIONS OF NIGGLI LATTICE I

Here we display general expressions in terms of the parameters a, σ, c, and d for the evaluation of Q_1 and $Q_{2,2}$ for Niggli Lattice I. The relations are meant to be illustrative of the methods used to calculate Q_1 and the $Q_{2,t}$ for various members of this class of plastically-deformed lattices.

Consider first the determination of $Q_1(\mathbb{P}_1)$ shown in Fig. 3. We may ascertain the content $\mathbb{P}_1^{(2)}$ of the asymmetric region $\mathbb{R}_1$ as follows. The area below the x axis is one-half the area of a regular hexagon of sides $2(a-\sigma)/\sqrt{3}$. This area is just $\sqrt{3}\,(a-\sigma)^2$. The area above the x axis is obtained upon ascertaining the equation of the line AB in a rectangular coordinate system. Given a function $f(x) =$ line AB, the area of interest is the area between the x axis and the line AB and between $+(a-\sigma)$ and $-(a-\sigma)$. Thus,

$$\mathbb{P}_1^{(2)} = \sqrt{3}\,(a-\sigma)^2 + \int_{-(a-\sigma)}^{(a-\sigma)} f(x)\,dx.$$

The position of a translated hexagonal lattice site P is parameterized by the variables c and d as shown in Fig. 3. The final parameterized expression for $\mathbb{R}_1^{(2)}$ attains the form,

$$\mathbb{P}_1^{(2)} = \sqrt{3}\,(a-\sigma)^2 + \int_{-(a-\sigma)}^{(a-\sigma)} (m_{AB}x - x_{AB}m_{AB} + y_{AB})\,dx$$

$$= \sqrt{3}\,(a-\sigma)^2 + 2(a-\sigma)[-x_{AB}m_{AB} + y_{AB}],$$

where m_{AB} is the slope of line AB and (x_{AB}, y_{AB}) represents the intersection of lines AB and OP of Fig. 3. Geometrically these may be determined solely in terms of the variables a, σ, c and d. Then $\mathbb{P}_1^{(2)}$ is entirely a function of a, σ, c and d and so represents a general solution for the limiting polytope bound to $Q_1(\mathscr{P}_1^{(2)})$ in terms of the variables which define the lattice distortion. The result above, derived in a rectangular coordinate system, may be expressed in terms of the oblique coordinate system used in earlier work [1, 2]. The Jacobian for the transformation is $\sqrt{3}/2$, thus, $Q_1 \cong \mathbb{P}_1^{(2)} = 3/2(a-\sigma)^2 + \sqrt{3}\,(a-\sigma)[-x_{AB}m_{AB} + y_{AB}]$.

The calculation of $Q_{2,2}$, one of the four correlated two-particle configurational partition functions, is considerably more complex. Figure 4 depicts this configuration. It is instructive to consider this specific calculation since it illustrates most of the problems encountered with this type of integration scheme.

We consider the sum of the following regions which comprise ($\mathbb{R}_{2,2}\mathbb{P}^{(4)}_{2,2}$):

(I) Region 1 correlated with Regions 4 and 5,

(II) Region 1 with Region 6,

(III) Region 2 with Region 5,

(IV) Region 2 with Region 6,

(V) Region 3 with Region 6.

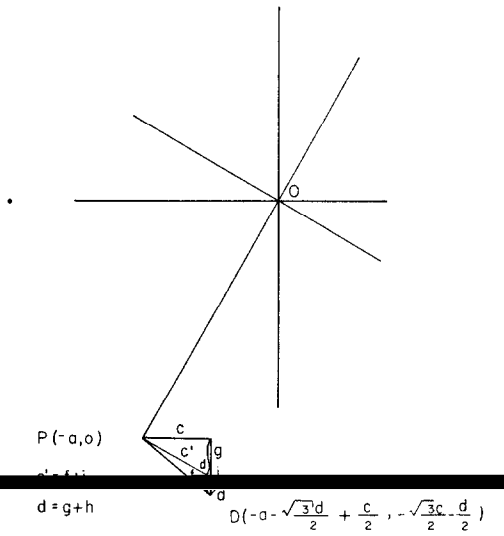

FIG. 8. Bound (e) for free area of Niggli Lattice I.

The sum of these five contributions with respect to the bounds denoted in Fig. 4 is $Q_{2,2}$. The configuration integrals for these regions are

$$I_1 = \left\{\frac{2}{\sqrt{3}}\left(-\frac{x_1^4}{8}T - \frac{x_1^3}{3}\left[\frac{S}{2} + T(a-\sigma)\right]\right.\right.$$

$$\left.\left. + \frac{x_1^2}{2}\left[TU - S(a-\sigma)\right] + SUx_1\right)\Big|_{x_1=n}^{x_1=d}\right\},$$

where

$$S = (2/\sqrt{3})(a-\sigma) + m_e x_e - y_e,$$

$$T = (1/\sqrt{3}) - m_e,$$

$$U = x_d^2/2 + 2(a-\sigma)\,x_d + (3/2)(a-\sigma)^2,$$

$$V = (-x_m^2/2)(1/m_e + 1/\sqrt{3}) + Tx_m + (a-\sigma)^2/2U + T(a-\sigma),$$

$$\mathrm{I}_2 = \frac{8}{3}\left[-\frac{x_1^3}{6} - \frac{x_1^2}{2}(a-\sigma) + \frac{3x_1}{2}(a-\sigma)^2\right]_{x_d}^{0},$$

$$\mathrm{II}_1 = \left[\frac{T}{2}x_1^2 + SX_1\right]_{x_n}^{x_d^2},$$

$$\mathrm{II}_2 = \frac{4(a-\sigma)}{1-\sqrt{3}\,m_e}\left[x_e m_e - y_e - \frac{2}{\sqrt{3}}(a-\sigma)\right]$$
$$\times\left[\frac{4\sqrt{3}\,T}{(1-3m_e)^2}(-x_e m_e + y_e)(a-\sigma) + \frac{2S(a-\sigma)}{1-\sqrt{3}\,m_e}\right]$$

$$\mathrm{II}_3 = \left[\frac{4(a-\sigma)}{\sqrt{3}}\left(-x_e m_e + y_e + \frac{2}{\sqrt{3}}(a-\sigma)\right)\frac{\sqrt{3}}{1-\sqrt{3}\,m_e}\right]$$
$$\times\left[\frac{-m_e}{(1-\sqrt{3}\,m_e)^2}(-x_e m_e + y_e)\left(\frac{2}{\sqrt{3}}(a-\sigma)\right) + \frac{4S(a-\sigma)}{1-\sqrt{3}\,m_e}\right],$$

$$\mathrm{II}_4 = \left[\frac{4}{\sqrt{3}}(a-\sigma)\,x_j\right]^2,$$

$$\mathrm{III} = \frac{11}{6}(a-\sigma)^4,$$

$$\mathrm{IV}_1 = 4\sqrt{3}\,(a-\sigma)^3\left[\frac{T(-x_e m_e + y_e)}{(1-\sqrt{3}\,m_e)^2} + \frac{S}{1-\sqrt{3}\,m_e}\right],$$

$$\mathrm{IV}_2 = 4x_j(a-\sigma)^3,$$

$$\mathrm{V}_1 = \left[\frac{-x_1^4}{8}U + \frac{x_1^3}{3}(2(a-\sigma)\,U + T)\right.$$
$$\left. + \frac{x_1^2}{2}[-V - 2(a-\sigma)\{(a-\sigma)U + T\}] + 2x_1 V(a-\sigma)\right]_{(a-\sigma)+x_j}^{2(a-\sigma)},$$

$$\mathrm{V}_2 = \frac{8}{3}(a-\sigma)\left\{\frac{x_1^3}{3} - \frac{x_1^2}{2}[3(a-\sigma) + x_j]\right.$$
$$\left. + 2(a-\sigma)[(a-\sigma) + x_j]\,x_1\right\}\Big|_{(a-\sigma)}^{(a-\sigma)+x_j},$$

where $m_e = -1/m_{OP}$ and (x_a, y_a),... are the coordinates at the points A,..., which are geometrically determined as functions of a, σ, c and d. Note again that, in terms of a, σ, c and d, the result is quite general and that by varying c and d we may consider $Q_{2,2}$ and the other $Q_{n,t}$ for a spectrum of distortions. It is quite difficult to consider such general higher-order correction terms, however. For example, $Q_{3,t}$ is much too complex to consider even for a polytope bound integration by computer inasmuch as the bounds themselves must be predetermined by the above analytic-geometric scheme for general distortions. The consequence of choosing specific values for a, σ, c and d, and so determining a numerical result for $Q_{2,1}$ and the other $Q_{2,t}$'s, is presented in the main text.

APPENDIX II: NIGGLI LATTICE II

Herein we explicitly characterize Niggli Lattice II which represents one extreme of the type of distortion (row translation) that is possible, i.e., maximal displacement allowable in the c direction. The approach is analogous to that employed for Niggli Lattice I as presented in Appendix I. The problem is greatly simplified, however, because of the increased symmetry inherent in this lattice. For example, in contrast to Niggli Lattice I there are only 3 distinct $Q_{2,t}$ subfigures to be considered. Moreover, the bounds of the single-particle "free areas" are greatly simplified, since by choosing a rectangular coordinate system where the axes

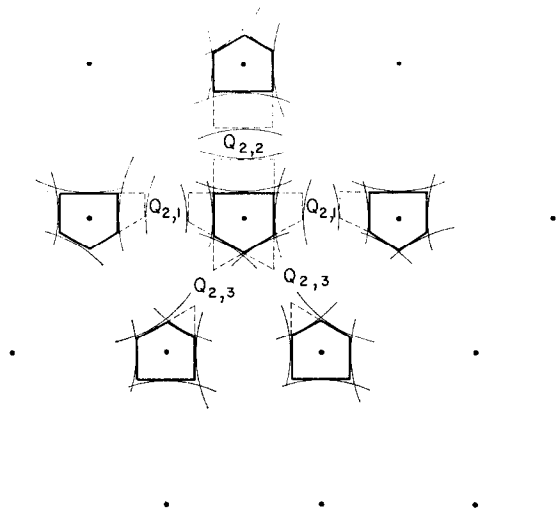

FIG. 9. Pair cell-clusters $Q_{2,t}$ of Niggli Lattice II.

include the disk centers the bases of the pentagonal "free areas" have zero slope. Also, dependence upon the variable (c) is eliminated, since the extremal nature of the distortion dictates that $c = \sigma/2$, where σ is the distance between disk centers. Further, by choosing a minimum value for (d), the distance from the center of a disk to the base of the pentagonal "free area" is $d = (a - \sigma)$, thus eliminating explicit dependence on (d) also.

$Q_1(\mathbb{P}_1^{(2)})$ is especially easy to evaluate and the result is completely analogous to that for Niggli Lattice I:

$$Q_1 \cong \mathbb{P}_1^{(2)} = 3/2(a - \sigma)^2 + \frac{2}{2}(a - \sigma)^2 = \frac{5}{2}(a - \sigma)^2.$$

Following the procedure of Appendix I we wish to display how a specific 2-particle configurational partition function obtains for Niggli Lattice II. Consider the configuration depicted in Fig. 9, denoted $\mathbb{R}_{2,1,II}(\mathbb{P}_{2,1,II}^{(4)})$ for which there are five constituent interactions given by the following five integrals:

I $$\int_{-(a-\sigma)}^{0} dx_1 \int_{A}^{a-\sigma} dy_1 \int_{-(a-\sigma)+x_1}^{0} dx_2 \int_{A'}^{a-\sigma} dy_2 ,$$

II $$\int_{-(a-\sigma)}^{0} dx_1 \int_{A}^{a-\sigma} dy_1 \int_{0}^{a-\sigma} dx_2 \int_{B'}^{a-\sigma} dy_2 ,$$

III $$\int_{0}^{a-\sigma} dx_1 \int_{B}^{a-\sigma} dy_1 \int_{-(a-\sigma)+x_1}^{0} dx_2 \int_{A'}^{a-\sigma} dy_2 ,$$

IV $$\int_{0}^{a-\sigma} dx_1 \int_{A}^{a-\sigma} dy_1 \int_{0}^{a-\sigma} dx_2 \int_{B'}^{a-\sigma} dy_2 ,$$

V $$\int_{a-\sigma}^{2(a-\sigma)} dx_1 \int_{B}^{a-\sigma} dy_1 \int_{-(a-\sigma)+x_1}^{a-\sigma} dx_2 \int_{B'}^{a-\sigma} dy_2 .$$

The bounds A and B are given by

$$A = y_1 = -(1/\sqrt{3})\, x_1 - (2/\sqrt{3})(a - \sigma),$$
$$B = y_1 = (1/\sqrt{3})\, x_1 - (2/\sqrt{3})(a - \sigma).$$

A' and B' are obtained from A and B by replacing x_1 with x_2 and y_1 with y_2. The specific evaluation of these integrals follows the procedure outlined in Appendix I. Numerical results obtained for specific values of a and σ are given in the main text.

APPENDIX III: BOUNDS TO LIMITING SUBFIGURES FOR NIGGLI CLOSE PACKINGS

Herein we wish to present a general prescription for constructing *bounds* to the limiting (high-density) subfigures for plastically-deformed Niggli close packings. While it is a straightforward procedure to construct the limiting subfigures for the regular hexagonal lattice, several ambiguities arise in the consideration of Niggli-type lattices such as we have considered here.

Ben-Naim and Stillinger [6] have definitively characterized the concept of a nearest neighbor for the construction of general Voronoi polyhedra. In order to illustrate the application of their criteria to Niggli-type lattices, consider Fig. 1. Voronoi polyhedra are constructed in the standard manner giving rise for Niggli Lattice I to the *asymmetric* hexagonal polytope and dual lattice network depicted in Fig. 1. The dual lattice consists of triangles and quadrilaterals. Moreover, each disk has 6 neighbors which fulfill the nearest neighbor criteria of Ref. [6]; i.e., adjacent Voronoi regions all have a common edge intersected by their line between centers. However, if we construct the *exact* cell-model, single-particle subfigure for Niggli Lattice I, we obtain a free area bounded by five arcs as shown in Fig. 10.

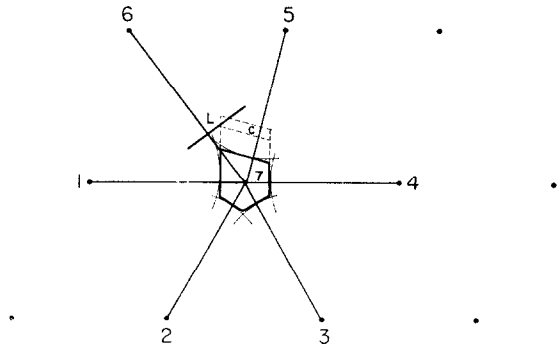

FIG. 10. Bound $\mathbb{R}_1^{(2)}$ ($\mathbb{P}_1^{(2)}$) to exact free area of Niggli Lattice I.

We cannot construct the high density, limiting subfigure corresponding to this exact region in a manner analogous to the regular hexagonal lattice, but a bound to this region may be so constructed. We thus observe that the content of the region $\Pi\mathbb{R}_1$, $\Pi\mathbb{P}_1^{(2)}$, is a bound to the content of the limiting polytope, $\mathbb{P}_1^{(2)}$, which is exact in the high-density limit; i.e., $\lim_{V\to V_0} \mathbb{P}_1^{(2)} = \mathscr{P}_1^{(2)}$ whereas $\lim_{V\to V_0} \Pi\mathbb{P}_1^{(2)} \approx \mathbb{P}_1^{(2)}$

(in the text we refer to the bounds by $\mathbb{P}$ only). In our construction Disk 6 is not considered to be a nearest-neighbor of Disk 7 inasmuch as the bound L contributed by the 6th disk is outside the free area defined by the other five interactions depicted in Fig. 10.

A two-particle subfigure is a representation of the additional free area accessible to a particle if a nearest-neighbor particle (with which it is correlated) is not restricted to remain at its nominal lattice site. For example, in Fig. 10, Disk 7 has access to the area depicted by the dashed lines if Disk 5 moves away from its lattice site to its extreme limit away from Disk 5, along the line $l_{5,7}$ drawn between lattice sites. With the extreme point along $l_{5,7}$ as center, a circle of radius σ intersects $l_{5,7}$ at point C. A line drawn through C perpendicular to $l_{5,7}$ defines the bound. Note that in some cases this bound will intersect line L. In such an event line L will become a bound of the two-particle subfigure even though it was not a bound of the one-particle free area.

APPENDIX IV: Exact Single-Particle Free Areas for Niggli Lattices

It is possible, by methods previously developed [1], to calculate the exact single-particle free areas for the Niggli Lattices. In practice, such calculations are tedious and are, in general, not carried out inasmuch as they are not able to be extended to higher order, i.e., beyond the approximation inherent in the cell model. We present them here for the sake of completeness.

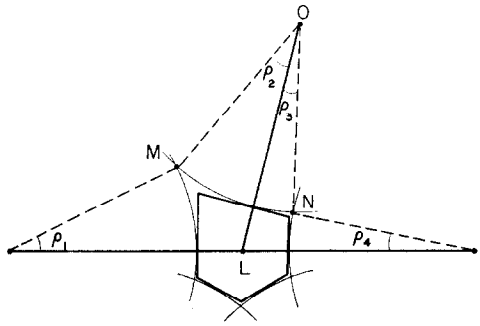

FIG. 11. Exact free area $\mathscr{A}_{1,1}^{(2)}(\mathscr{P}_{1,1}^{(2)})$ for Niggli Lattice I.

Niggli Lattice I

$$Q_{1,I}(\mathscr{P}^{(2)}_{1,I}) = \tfrac{1}{2}Q_1(\mathscr{P}^{(2)}_1), \text{ hexagonal} + \tfrac{1}{2}[a\sigma \sin \rho_1 + \sigma L \sin \rho_2 + \sigma L \sin \rho_3 + a\sigma \sin \rho_4 - \sigma^2(\rho_1 + \rho_2 + \rho_3 + \rho_4)],$$

where

$$Q_1(\mathscr{P}^{(2)}_1), \text{ hexagonal} = \sigma^2\{(3\sqrt{3}/2)\,\tau_\sigma - 3[\tau_\sigma(1 - \tau_\sigma/4)]^{1/2} - 2\pi + 6\cos^{-1}(\tau_\sigma/2)\},$$

$$\tau_\sigma = a^2/\sigma^2,$$

$$L = [(a/2 - c)^2 + (\sqrt{3}\,a/2 + d)^2]^{1/2},$$

$$\rho_1 = \cos^{-1}(\sigma^2 + a^2 - D^2_{LM}/2a\sigma),$$

$$\rho_2 = \cos^{-1}(\sigma^2 + L^2 - D^2_{LM}/2a\sigma),$$

$$\rho_3 = \cos^{-1}(\sigma^2 + L^2 - D^2_{LN}/2a\sigma),$$

$$\rho_4 = \cos^{-1}(a^2 + \sigma^2 - D^2_{LN}/2a\sigma).$$

Refer to Fig. 11 for an illustration of these parameters.

Niggli Lattice II

$$Q_{1,II}(\mathscr{P}^{(2)}_{1,II}) = \tfrac{1}{2}Q_1(\mathscr{P}^{(2)}_1), \text{ hexagonal} + 2(\sigma a \sin \rho_5 - \sigma^2\rho_5),$$

where

$$\rho_5 = \cos^{-1}(a^2 + \sigma^2 - D^2/2a\sigma)$$

and D is defined in Fig. 12.

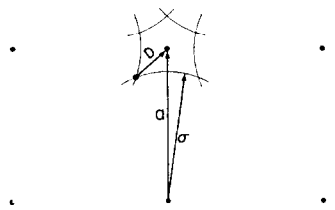

FIG. 12. Parameters defining exact free area $\mathscr{P}^{(2)}_{1,II}$ ($\mathscr{P}^{(2)}_{1,II}$) of Niggli Lattice II.

REFERENCES

1. C. G. MILLER AND R. D. LARSEN, "Exact Cell and Correlated-Cell Model Molecular Pair Distribution Functions," Special Technical Report No. 1, Project THEMIS, Illinois Institute of Technology, Chicago, June 1970.
2. F. H. STILLINGER, JR., Z. W. SALSBURG, AND R. L. KORNEGAY, *J. Chem. Phys.* **43** (1965), 932.
3. W. G. RUDD, Z. W. SALSBURG, A. P. YU AND F. H. STILLINGER, JR., *J. Chem. Phys.* **49** (1968), 4857.
4. Haag has depicted many interesting varieties of disk close packings in F. HAAG, *Zeits. fur Krist.* **70** (1929), 353. Haag refers to them as Niggli Close Packings and we retain that nomenclature herein.
5. W. G. RUDD, Z. W. SALSBURG AND L. MASINTER, *J. Comp. Phys.* **5** (1970), 125.
[redacted]
Laboratories Technical Report, Murray Hill, N. J., unpublished.